Green Chemistry

Elucidating the mechanisms of enhanced lignin bioconversion by an alkali sterilization strategy

Journal:	*Green Chemistry*
Manuscript ID	GC-ART-03-2021-000911.R1
Article Type:	Paper
Date Submitted by the Author:	21-Apr-2021
Complete List of Authors:	Zhao, Zhi-min; University of Tennessee Knoxville College of Engineering Zhang, Shuyang; University of Tennessee Knoxville College of Engineering, Meng, Xianzhi; University of Tennessee, Pu, Yunqiao; Oak Ridge National Laboratory, Joint Institute of Biological Science, Biosciences Division Liu, Zhi-Hua; Tianjin University Ledford, William; University of Tennessee Knoxville College of Engineering Kilbey, S.; University of Tennessee Knoxville College of Engineering, Chemistry Li, Bing-Zhi; Tianjin University; Tianjin University, Ragauskas, Arthur; University of Tennessee Knoxville College of Engineering

Elucidating the mechanisms of enhanced lignin bioconversion by an alkali sterilization strategy

Zhi-Min Zhao,[a,b] Shuyang Zhang,[b] Xianzhi Meng,[b] Yunqiao Pu,[c] Zhi-Hua Liu,[d] William K. Ledford,[e] S. Michael Kilbey II,[b,e] Bing-Zhi Li[d] and Arthur J. Ragauskas*[b,c,f]

[a] *School of Ecology and Environment, Inner Mongolia Key Laboratory of Environmental Pollution Control & Wastes Reuse, Inner Mongolia University, Hohhot, 010021, China*

[b] *Department of Chemical & Biomolecular Engineering, University of Tennessee Knoxville, Knoxville, TN 37996, USA*

[c] *Joint Institute of Biological Science, Biosciences Division, Oak Ridge National Laboratory (ORNL), Oak Ridge, TN 37831, USA*

[d] *Frontiers Science Center for Synthetic Biology and Key Laboratory of Systems Bioengineering (Ministry of Education), School of Chemical Engineering and Technology, Tianjin University, Tianjin, 300072, China*

[e] *Department of Chemistry, University of Tennessee Knoxville, Knoxville, TN 37996, USA*

[f] *Department of Forestry, Wildlife, and Fisheries, Center for Renewable Carbon, University of Tennessee Institute of Agriculture, Knoxville, TN 37996, USA*

** Corresponding author: Arthur J. Ragauskas; E-mail address: aragausk@utk.edu*

Abstract

Biological lignin valorization represents an emerging green approach to upgrade lignin for sustainable and economic biorefineries. However, lignin generally exhibits poor water solubility and inhomogeneous distribution in an aqueous medium, significantly limiting its bioconversion efficiency. Herein, we develop a novel alkali sterilization strategy to effectively enhance the dispersion and fermentation performance of lignin substrates. The colloidal particle size and molecular structure variations of lignin during the sterilization were thoroughly investigated to reveal the mechanisms of enhanced fermentation performance. Results showed that alkali sterilization achieved a completely aseptic effect when mixing lignin medium at an initial pH 12.7 for 24 h. Dynamic light scattering (DLS) analysis demonstrated that the volume of colloidal lignin particles decreased by 96.3% by alkali sterilization compared with the conventional thermal sterilization. Moreover, lignin characterizations by nuclear magnetic resonance (NMR) and gel permeation chromatography (GPC) suggested that alkali sterilization modified lignin molecular structure by generating 50% more hydrophilic carboxyl groups, reducing the weight-average molecular weight (M_w) by 23.0%, and narrowing the molar-mass dispersity ($Đ_M$) by 23.8%. The generation of lignin substrates with more uniform distribution and lower molecular weight improved *Rhodococcus opacus* PD630 cell growth and metabolism synchronously. Microbial cell amount, lignin degradation, and lipids production in alkali sterilized medium increased by 309%, 30.3%, and 48.3%, respectively, compared to those in thermally sterilized medium. These results clearly demonstrated that alkali sterilization dramatically improved the lignin bioconversion performance. This work presents a facile and effective sterilization strategy to overcome inhomogeneous lignin distribution in aqueous fermentation mediums, showing great potentials as a platform technique for promoting biological lignin valorization.

Keywords: alkali sterilization, lignin bioconversion, lignin dispersion, *Rhodococcus opacus* PD630, lipids, lignocellulosic biomass

1. Introduction

Lignin constitutes 15 to 40% of the dry weight of most terrestrial plants[1-3] and is the second most abundant natural polymer on earth after cellulose.[4-6] Lignin valorization is considered an essential process for realizing sustainable and economic biorefineries based on techno-economic analyses.[7-10] In nature, lignin is an amorphous three-dimensional aromatic polymer composed of phenylpropane units cross-linked via various ether linkages and carbon-carbon bonds, including aryl ether (*β*-O-4), phenylcoumaran (*β*-5), biphenyl (5-5), resinol (*β*-*β*), and diaryl ether linkage (4-O-5).[11,12] Besides, native lignin structure varies from plant species and technical lignin streams further demonstrates significant diversity after different fractionation treatments of lignocellulose, such as Kraft pulping and Organosolv processes.[13] The heterogeneity of lignin presents a significant barrier to its upgrading utilization regardless of the applied strategies.[14] Biological lignin valorization is emerging as a promising platform for lignin conversion since natural microbial conversion processes can funnel aromatic mixtures to value-added chemicals (e.g., lipids,[15-19] polyhydroxyalkanoate,[20-23] and muconic acid[24-26]). The process shows great advantages of overcoming lignin heterogeneity.[14,18,27] Meanwhile, lignin conversion through biological platform harnesses the natural catalytic power of microorganisms to decompose complex lignin molecules, representing a green approach under mild operation conditions without intensive energy input.[14, 28-30]

Mass transfer is one of the major concerns in chemical reaction processes and undoubtedly is a determining factor for biochemical process efficiency as well.[31] A sufficient contact between substrates and microbial cells is a prerequisite for high efficiency fermentations.[32] However, owing to the intrinsic heterogeneity of its complex structure, lignin generally exhibits poor water solubility, frequently resulting in an inhomogeneous lignin distribution in aqueous fermentation mediums.[33,34] The relatively poor lignin dispersion in the medium has become one of the major challenges limiting lignin's biological conversion efficiency.[10,35] Many efforts have been directed to improve lignin's distribution in fermentation mediums from the aspects of tailoring lignin chemical structure and developing advanced processes.[34] For example, cosolvent enhanced lignocellulosic fractionation (CELF)[36-38] and acid-alkali combinatorial

pretreatment[39-42] had been designed to modify lignin chemistry by reducing the molecular weight and generating more hydrophilic groups (e.g., carboxyl groups). These modified lignin structures could benefit from improving their distribution uniformity in an aqueous medium and further facilitating fermentation performance.[39,40] Meanwhile, alkaline solubilization approach can be used to improve lignin dispersion since it could alter colloidal lignin particles' charge and avoid lignin colloid coagulation.[30,43] Previous studies[15,44,45] showed that adjusting lignin-containing medium to pH 12.0 can dissolve the lignin powder, following neutralization of the medium to pH 7.0-7.5, the lignin medium can be used for fermentation. Through these efforts, the uniformity of lignin distribution in the fermentation medium could be improved effectively. However, sterilization for fermentation medium is an essential operation to ensure pure culture. Moist heat sterilization has been widely used in fermentation due to its reliable sterilization effect and readily available steam.[46] Heat treatment during the thermal sterilization could alter lignin structure and further reduce the lignin distribution uniformity in the fermentation medium. It was reported that condensation reactions occurred during the heat sterilization process,[47-49] which might cause aggregation of lignin particles. Therefore, due to the intrinsic structure of lignin and the necessity of sterilization operation, improving lignin distribution in fermentation mediums remain as a major challenge facing biological lignin valorization.[10,35]

Solution pH plays an important role in affecting microbial metabolism. Most microbes cannot survive in an extreme pH environment. Therefore, alkali can also be applied for sterilization because a high concentration of hydroxide ions could lead to denaturation and deactivation of biological macromolecules (i.e., proteins, nucleic acids).[46,50] Spores of *Bacillus* and *Clostridium* species have long been known to be resistant to various sterilization methods.[51,52] However, with alkaline sterilization at 1 M NaOH, 99.99% of *B. subtilis* cells were killed in 1 min while 90% of spores could not survive within 60 min.[50] Further studies revealed that the apparent spore killing caused by alkali treatment is due to the inactivation of crucial spore cortex lytic enzymes.[50] These results indicated the efficient sterilization could be achieved by alkali

treatment.

Since alkali could facilitate lignin dispersion and be used in sterilization operation, we hypothesized that alkali sterilization could be applied to replace thermal treatment for lignin medium to improve lignin distribution while yielding a pure culture. Meanwhile, the issue of how alkali sterilization could potentially influence fermentation performance remained uncertain. To address these issues, a multi-target alkali sterilization strategy for lignin medium was developed in the present study, and its comprehensive influence on fermentation efficiency was evaluated. Firstly, sterilization effects by alkali, conventional moist heat, and a combination of these two methods were examined. Alkali treatment conditions for complete sterilization were determined. Colloidal lignin particle size distribution was then characterized by applying dynamic light scattering (DLS) to clarify the lignin dispersion from different sterilization methods. Moreover, lignin molecular weight and chemical structure were analyzed using gel permeation chromatography (GPC) and nuclear magnetic resonance (NMR) spectroscopy before and after different types of sterilization treatments. Finally, fermentation efficiency was examined by employing *Rhodococcus opacus* PD630 to produce lipids utilizing the different sterilized mediums. The mechanisms for improved lignin utilization and enhanced fermentation performance by alkali sterilization were proposed.

2. Experimental

2.1 Fermentation medium preparation with different sterilization treatment

A commercial softwood Kraft lignin sample was purified following a published methodology.[53] In brief, 100 g of dry Kraft lignin was first suspended in 1000 mL of 0.1 M NaOH solution with EDTA-2Na$^+$ (0.5% w/v). The mixture was then filtrated through a filter paper (Whatman 1). The filtrate was acidified gradually to pH 3.0 with 2 M H_2SO_4 and then stored at −20 °C overnight. After thawing, the precipitates were collected by centrifugation and washed thoroughly with deionized water. The obtained air-dried lignin powder was used in the following fermentation. The fermentation

medium contains *Rhodococcus* minimal (RM) medium and lignin as the sole carbon source. The RM medium contains (per liter): 1.4 g $(NH_4)_2SO_4$, 1.0 g $MgSO_4 \cdot 7H_2O$, 0.015 g $CaCl_2 \cdot 2H_2O$, 1.0 mL trace element solution, 1.0 mL stock A solution, and 35.2 mL phosphate buffer (1.0 M, pH 7.0). Where the trace element solution contains 0.050 g/L $CoCl_2 \cdot 6H_2O$, 0.005 g/L $CuCl_2 \cdot 2H_2O$, 0.25 g/L EDTA, 0.50 g/L $FeSO_4 \cdot 7H_2O$, 0.015 g/L H_3BO_3, 0.020 g/L $MnSO_4 \cdot H_2O$, 0.010 g/L $NiC1_2 \cdot 6H_2O$, and 0.40 g/L $ZnSO_4 \cdot 7H_2O$. Stock A solution was composed of 5.0 g/L FeNa-EDTA and 2.0 g/L $NaMoO_4 \cdot H_2O$.[15,54] Chemicals were purchased from Sigma-Aldrich and Fisher Scientific and used as received.

1.5 g Kraft lignin and 150 mL of RM medium were mixed in 250 mL Erlenmeyer flasks, and the mixture was shaken at 180 rpm for 15 min. After that, the medium was adjusted to pH 12.7 with 10 M NaOH. As shown in Fig. 1, one group of mediums was shaken at 180 rpm for 30 min to dissolve the lignin powder as described in previous studies.[15,44] The other group was shaken at 180 rpm for 24 h, aiming to not only improve lignin dispersion but also achieve a complete sterilization by alkaline treatment. Then the pH of all samples were adjusted to 7.2 with 4 M HCl under aseptic conditions. Prior to fermentation, one sample from each group was subjected to conventional moist heat sterilization (121 °C, 20 min) using an autoclave as the control.

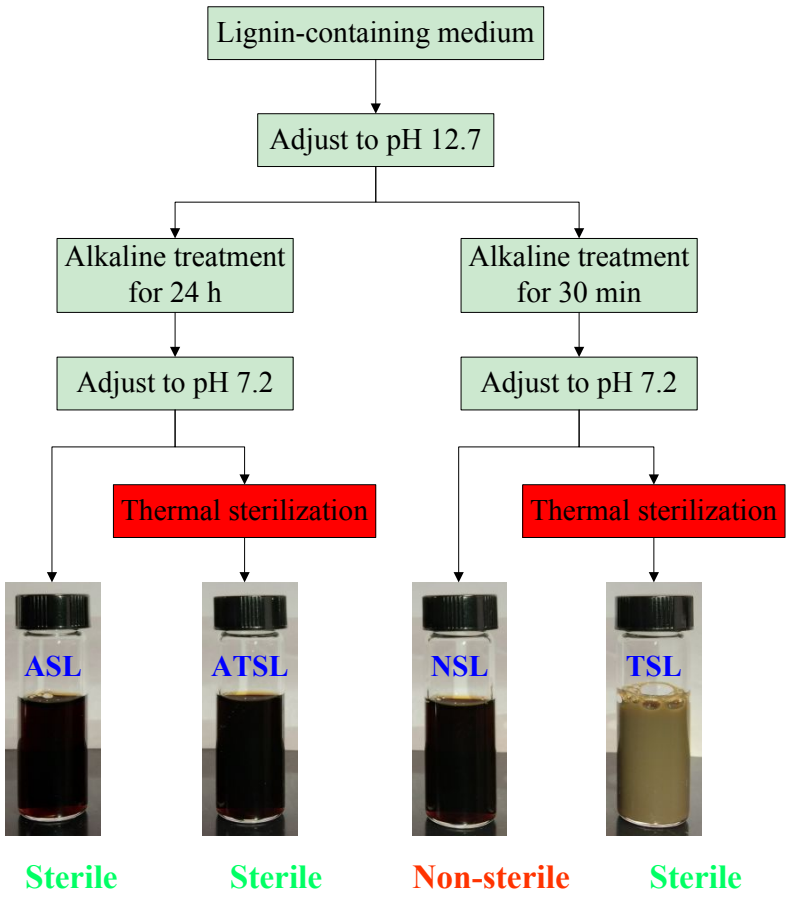

Fig. 1 Flowchart of different sterilization treatments of lignin-containing medium. ASL: alkaline sterilized lignin, ATSL: alkaline and thermally sterilized lignin, NSL: non-sterilized lignin, TSL: thermally sterilized lignin.

2.2 Sterilization efficiency of different treatments for lignin medium

The spread plate (SP) method was applied to evaluate the aseptic effect of lignin mediums with different treatments. 100 μL samples of different mediums were taken under sterile conditions and then spread over LB agar plates' surface. After incubation at 28 °C for 72 h, the colony-forming units (CFU) were examined to evaluate the sterilization effect by different sterilization treatments.

2.3 Lignin distribution in a sterilized medium characterized by dynamic light scattering (DLS)

Generally, Kraft lignin tends to form a colloid structure in an alkaline solution and thus distributes relatively uniformly in the aqueous medium.[43] Adjusting lignin medium to alkaline and then neutral help maintain the colloid structure in medium,[15,44] whereas

the heat treatment alters lignin structure. In order to investigate the influence of different sterilization treatments on lignin dispersion in medium, DLS was applied to determine the colloidal lignin particle size distribution. 3.0 mL of lignin medium after sterilization was sampled and centrifuged at 10000 rpm for 10 min to separate the precipitates that might form during the heat treatment. The supernatant was subjected to DLS measurements using a four-detector, goniometer-based ALV Light Scattering System equipped with a 22 mW He-Ne laser (wavelength, λ=632.8 nm), which includes an ALV-7004 Multiple Tau Digital Correlator for signal processing to generate a normalized light intensity autocorrelation function at each scattering angle. Consistent with methods described in our prior works,[55-57] autocorrelation functions were analyzed by the CONTIN algorithm to determine the distribution of decay rates, which provides insight into the distribution of hydrodynamic sizes of the scatterers present in solution. The solids (if any) after centrifugation were lyophilized to measure the weight of lignin precipitates during sterilization processes.

2.4 Fermentation experiment using lignin as a carbon source

R. opacus PD630 strain (DSMZ 44193) was purchased from the German Collection of Microorganisms and Cell Cultures (DSMZ, Braunschweig, Germany). The seed culture was prepared by inoculating a single colony of *R. opacus* PD630 (hereafter PD630) into 80 mL Tryptic Soy Broth (TSB) medium and cultivated with a shaking speed of 180 rpm for approximately 24 h to an OD_{600} value of 1.5. The cultured cells were then harvested by centrifuging and washing twice with 80 mL of sterile 0.85% (w/v) NaCl solution and resuspended in a 80 mL of 0.85% (w/v) NaCl solution. The seed solution was inoculated into the lignin-containing medium with an inoculation dose of 5% (v/v). Fermentation was conducted in 250 mL Erlenmeyer flasks and incubated in a shaker at 180 rpm, 28 °C for 7 days.

2.5 Measurement of microbial growth and lipids yield

The serial dilution plate (SDP) method was applied to track PD630 cell growth during fermentation. 0.1 mL of fermentation medium was serial diluted and plated for 10^4 dilutions. The numbers of colonies were determined and expressed as CFU/mL. For

lipids content analysis, 30 mL of fermentation broth was sampled and adjusted to pH 12.7 with 10 M NaOH to dissolve lignin. Then the sample was centrifuged at 5000 rpm for 10 min. The supernatant (*S*) was collected for further analysis. The pelleted cells were washed by 30 mL of sterile 0.85% (w/v) NaCl and then lyophilized in a vacuum freeze-dryer (Labconco FreeZone 2.5L, USA). After lyophilization, the cell pellets were suspended with 20 mL methanol at 65 °C for 30 min. 1.0 mL of 10 M NaOH was added and incubated at 65 °C for 2 h. Then the sample was moved from the water bath and cooled to room temperature. 1.0 mL of 98% (w/w) H_2SO_4 was added drop by drop and incubated in 65 °C water bath for another 2 h. After which, the solution was cooled to room temperature, 8.0 mL hexane was added and incubated with periodic shaking for 5 min to extract lipids. The top hexane layer was collected in a pre-weighed glass vial (weight recorded as W_1) after centrifugation at 5000 rpm for 10 min, and this hexane extraction step was repeated once more. The top hexane layer was again transferred into the previous glass vial and then dried to constant weight (weight recorded as W_2). The lipids production utilizing lignin as the sole carbon source was calculated as follows:

$$\text{Lipids concentration} = (W_2 - W_1)/0.03 \text{ (mg/L)} \quad (1)$$

2.6 Characterization of lignin properties during fermentation

2.6.1 Lignin concentration determined by UV/Vis

30 mL of fermentation broth was sampled and adjusted to pH 12.7 with 10 M NaOH to dissolve lignin. Then the sample was centrifuged at 5000 rpm for 10 min. 0.1 mL of supernatant *S* was taken for lignin concentration determination using a UV/Vis spectrophotometer (UV160U, Shimadzu, Japan) at a wavelength of 300 nm with appropriate dilution.[58,59] A standard calibration curve was established with the same reagents and known concentration of Kraft lignin. Lignin concentration was then calculated according to the standard curve function. Based on the lignin concentration changes, lignin degradation during fermentation was determined as the equation below[54]:

$$\text{Lignin degradation} = \left(1 - \frac{\text{lignin concentration after fermentation}}{\text{lignin concentration before fermentation}}\right) \times 100\% \quad (2)$$

2.6.2 Lignin molecular weight characterization by gel permeation chromatography (GPC)

The supernatant *S* was adjusted to pH 2.0 to precipitate lignin. The sample was then centrifuged at 5000 rpm for 10 min, and the precipitated lignin was lyophilized to constant weight. The lyophilized lignin samples (~5 mg) were acetylated with a 2.0 mL acetic anhydride/pyridine (1:1, v/v) mixture for 24 h at room temperature. 5.0 mL ethanol was added to the reaction and left for 30 min. Then the solvent was subjected to rotary evaporation under reduced pressure. The whole process was repeated twice until the acetic acid was completely removed. Then the derivatized lignin was dissolved in tetrahydrofuran (THF) at a concentration of 1 mg/mL. The solution was filtered through a 0.45 μm PTFE filter prior to GPC analysis. The molecular weight analysis was conducted on an Agilent GPC SECurity 1200 system equipped with a UV detector. THF was used as the mobile phase at a flow rate of 0.5 mL/min. The injection volume was set at 50 μL. Polystyrene standards of narrow molecular weight were used to prepare a calibration curve. The weight-average molecular weight (M_w) and molar-mass dispersity ($Đ_M$) of lignin were calculated using WinGPC Unity software.[38]

2.6.3 Lignin structure analysis by nuclear magnetic resonance (NMR)

Two-dimensional ^{13}C-^{1}H HSQC and ^{31}P NMR were employed to analyze lignin structure with a Bruker Avance III HD 500-MHz spectrometer. The lyophilized lignin samples (~50 mg) were dissolved in 0.6 mL of DMSO-d_6. HSQC experiments were performed with a Bruker pulse sequence (hsqctgpspsi2.2) using an N_2 cryoprobe (BBO ^{1}H & ^{19}F-5 mm) under the following conditions: 166 ppm spectral width in F1 (^{13}C) dimension with 256 data points (acquisition time 6.1 ms) and 12 ppm spectral width in F2 (^{1}H) dimension with 1024 data points (acquisition time 85.2 ms), a 1.0 s delay, a $J_{C\text{-}H}$ of 145 Hz, and 128 scans. As for ^{31}P NMR analysis, the oven dried lignin samples (~20 mg) were dissolved in a solvent mixture of pyridine and deuterated chloroform (1.6/1.0, v/v, 0.50 mL). The solution was then derivatized with 0.075 mL of 2-chloro-4,4,5,5-tetramethyl-1,3,2-dioxaphospholane (TMDP). Chromium acetylacetonate and

endo-N-hydroxy-5-norbornene-2,3-dicarboximide (NHND) were added as the relaxation agent and internal standard, respectively. Quantitative ^{31}P NMR spectra of phosphitylated lignin were acquired using an inverse-gated decoupling pulse sequence (Waltz-16), 90° pulse, 25 s pulse delay with 64 scans.[60,61] All the data was processed using the TopSpin 4.1.0 software (Bruker BioSpin).

2.7 Fermentation metabolites of lignin detected by gas chromatography-mass spectrometry (GC-MS)

The degradation metabolites of lignin in fermentation broth were determined by using GC-MS. 10 mL of ethyl acetate was added to 5 mL of fermentation broth sample in a 50 mL centrifuge tube and was vortexed for 5 min at room temperature. The top ethyl acetate layer was collected and vortexed with 7 mL of ethyl acetate for another 5 min. The collected ethyl acetate layer was then subjected to rotary evaporation under reduced pressure at 30 °C. The sample was then resuspended in 1.0 mL of ethyl acetate and determined using Agilent 7890A-5975C GC-MS with an HP-5ms capillary column (30 m × 0.25 mm id, film thickness 0.25 μm). Helium was used as the carrier gas at a flow rate of 1.5 mL/min. The injection volume was set at 1 μL and in the splitless mode. The oven temperature was maintained at 50 °C for 5 min and raised to 300 °C at 20 °C/min. Compounds were identified by comparison of their mass spectra with the standard spectra in the NIST (National Institute of Standards and Technology) library.

3. Results and discussion

3.1 Sterilization effect of lignin medium after different sterilization treatment

Sterilization of the medium is essential to ensure pure culture, influencing target strain growth and fermentation performance.[46] Prior to fermentation by PD630, the aseptic effect of lignin-containing medium was examined for different sterilization treatments. Moist heat at 121 °C for 20 min achieved a complete sterilization in ATSL and TSL mediums as expected, which was confirmed by the spread plate (SP) method. Meanwhile, it was found that ASL medium mixed at initial pH 12.7 for 24 h was completely sterile (Fig. S1). In fact, strong alkali is a kind of effective sterilization

reagent due to the denaturation and deactivation of biological macromolecules caused by the high concentration of hydroxide ions.[50] However, alkali sterilization has not been widely used in fermentation compared with moist heat sterilization. One main drawback, similar to other chemical disinfectants, is that alkali sterilization brings additional chemicals to the medium, which might cause contamination to the substrates.[46,62] For lignin bioprocessing, sodium hydroxide is generally added to the medium to dissolve lignin powder for improving its distribution uniformity.[15,44] After alkali treatment, the medium was neutralized with HCl to pH 7.0-7.5 for microbial growth. The resulting concentration of NaCl approximately equaled 0.85%, which fell within the concentration range of normal saline that was suitable for microbial growth. Therefore, there is no need to concern about the possible contamination of the lignin medium and high salt inhibition effect caused by the alkali sterilization strategy used in the present study. On the other hand, it was noticed that colonies of contaminating microbes appeared on the plate surface of NSL medium (Fig. S1), illustrating the incomplete sterilization through mixing at initial pH 12.7 for 30 min. This might be due to the inadequate alkali treatment time for NSL medium. Overall, it was confirmed that complete sterilization was achieved in ASL medium by mixing at initial pH 12.7 for 24 h, demonstrating alkali sterilization could be an effective sterilization method for lignin-containing medium.

3.2 Colloidal lignin particle size distribution in different mediums

Generally, Kraft lignin disperses in an alkaline solution to form a colloid structure.[43] As shown in equations (3) and (4), the colloidal lignin particles with a negative charge in an alkaline environment were attributed to the carboxylic acid and phenolic hydroxyl groups. These negatively charged colloidal particles repel each other by electrostatic interactions and thus keep the medium stable.[43,63,64]

$$\text{-COOH} + \text{OH}^- \rightleftharpoons \text{-COO}^- + \text{H}_2\text{O} \quad (3)$$

$$\text{Ar-OH} + \text{OH}^- \rightleftharpoons \text{Ar-O}^- + \text{H}_2\text{O} \quad (4)$$

Solution pH plays a significant role in the formation of lignin dispersion.[63] To promote

lignin solubilization in the fermentation medium, pH was usually adjusted above 12.0 to dissolve lignin powder and then neutralized to 7.0-7.5 for microbial growth.[15,44] Through these operations, the lignin colloid structure was formed under the alkaline conditions and was then maintained at pH 7.0-7.5.[43] Fig. 2 shows the pH changes during these adjusting processes. It is worth noting that pH values were continuously decreasing during the mixing process for 24 h. This phenomenon suggests that the ionization of acidic groups (i.e., -COOH and Ar-OH) within lignin medium had not reached an equilibrium state, even though the lignin powder had been dissolved rapidly within 30 min under the alkaline condition. Acidic groups such as -COOH and Ar-OH were consuming OH^- as shown in equations (3) and (4), which led to the pH decrease during this mixing process. Accordingly, more anions such as $-COO^-$ and $Ar-O^-$ were generated with the OH^- consumption. As a result, colloidal lignin particles were more negatively charged, and the electrostatic interactions between them became stronger, which should facilitate lignin distributing more uniformly. It was also noted from Fig. 2 that pH decreased rapidly during the first 30 min mixing while the decreasing speed slowed down as the mixing process prolonged, which might be due to that the forward reactions in equations (3) and (4) became slowly as the OH^- were consumed. As a result, pH values of ASL and ATSL mediums decreased from an initial 12.7 to 12.3 during the mixing process for 24 h while the pH of NSL and TSL mediums decreased to 12.6 after mixing for 30 min.

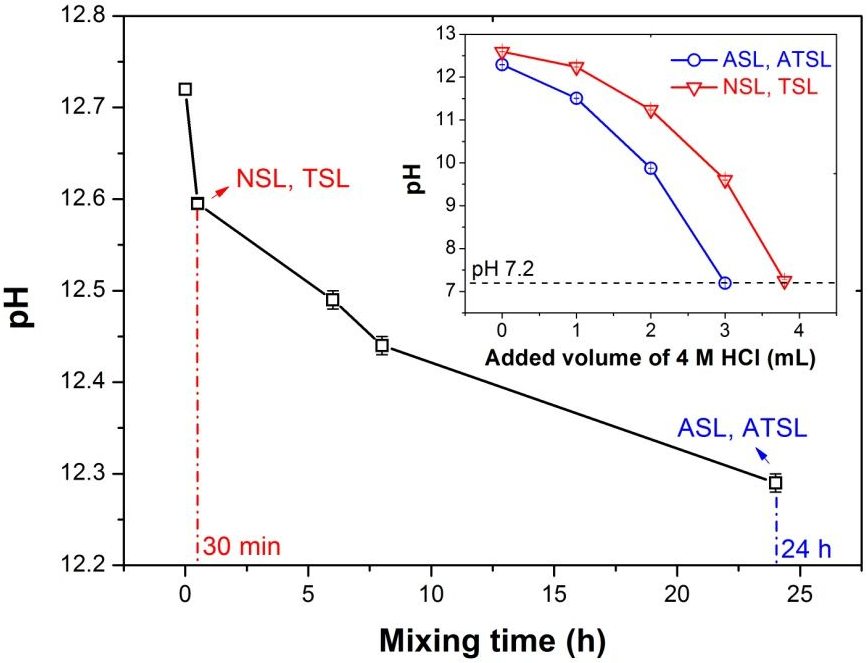

Fig. 2 pH changes during mixing lignin-containing medium at initial pH 12.7 and the subsequent neutralizing process by adding HCl. The data represent the average of two replicates. Error bars represent standard deviations.

Prior to fermentation, the pH of the mediums should be adjusted for microbial growth as the optimal pH condition is around 7.0-7.5.[15,39] As shown in Fig. 2, the pH of ASL and ATSL mediums reduced rapidly with HCl addition compared with those of NSL and TSL mediums. Meanwhile, the pH of ASL and ATSL reached 7.2 by adding 3.0 mL of 4 M HCl, while the amount of HCl needed for NSL and TSL was 3.8 mL. These phenomena also indicated that more OH^- were consumed by -COOH and Ar-OH in ASL and ATSL mediums during a longer mixing process. To conclude, these results demonstrated that acidic group ionization reactions in the alkaline environment were ongoing during the mixing process for 24 h. Therefore, as the mixing period prolonged from 30 min to 24 h, the more negatively charged lignin molecular structure strengthened electrostatic repulsion, which should avoid colloidal lignin particles aggregation and enhance the colloidal stability.

Fig. S2 shows the sample images of lignin medium after different sterilization

treatments. It was found that the color of TSL medium was obviously different from others, suggesting that the thermal sterilization at 121 °C for 20 min altered lignin medium properties significantly, especially for the medium treated by alkali for a relatively short time (i.e., 30 min). Although ATSL also underwent thermal sterilization, its color was more similar to ASL and NSL. The possible reason for these phenomena was that thermal treatment altered chromophore structures (e.g., *ortho*- and *para*-quinones) in TSL, resulting in a significantly different color comparing with other mediums.[65,66] While for ATSL, since the ionization of acidic groups occurred more sufficiently during the longer alkali treatment process (i.e., 24 h), the stability of colloidal lignin structure was effectively improved. As a result, ATSL presented a stronger resistance to the thermal treatment and showed different properties compared to TSL. On the other hand, the light transmittance results demonstrated that ATSL and TSL with thermal sterilization were less transparent than ASL and NSL, suggesting non-negligible effects of thermal sterilization on altering lignin structure and dispersion. Considering the influence of alkali treatment time on lignin distribution, it was noticed that the light transmittance of ASL was better than NSL. This result also suggests that prolonging the mixing process at alkaline conditions should facilitate the generation of smaller colloidal lignin particles and more uniform lignin distribution.

The precipitation behavior of lignin in different mediums upon different sterilization treatment was examined. As shown in Table 1, there was no precipitate generation in ASL and NSL mediums. This could be explained by that H^+ added to these mediums during the neutralization process was preferentially reacted with free OH^-. As a result, most negative ions such as $-COO^-$ and $Ar-O^-$ were maintained, hindering the aggregation of colloidal lignin particles. However, in ATSL and TSL mediums that underwent thermal sterilization, lignin precipitates were formed. Especially for TSL, the lignin precipitates accounted for 20.5% weight of the whole lignin substrates. These results confirmed that the thermal sterilization caused lignin particle aggregation while prolonging mixing time in an alkaline environment could efficiently reduce the aggregation effect caused by the thermal sterilization.

Table 1. Precipitates weight percentage in lignin medium after different sterilization treatment

Samples	ASL	ATSL	NSL	TSL
Alkaline treatment time	24 h	24 h	30 min	30 min
Thermal sterilization	No	Yes	No	Yes
Complete sterilization	Yes	Yes	No	Yes
Precipitates weight percentage (%)[a]	ND	1.34 ± 0.05	ND	20.5 ± 0.2

[a] ND: not detected. Data are means ± standard deviations of two replicates.

To further characterize lignin dispersion, DLS measurements were used to assess the size distribution of colloidal lignin particles in different mediums. As shown in Fig. 3, different samples demonstrated significant variations in colloidal particle size distribution. ASL and TSL mediums before fermentation presented relatively narrow distributions, implying relatively uniform colloidal lignin particle sizes. The peak value of the hydrodynamic radius of TSL before fermentation was 45 nm, which was 3-fold larger than that of ASL. This result revealed that thermal sterilization led to aggregation of lignin particles, increasing the size of the colloidal particles and even causing precipitation. As for ATSL before fermentation, the peak was multimodal, possibly due to that mixing at the alkaline condition for 24 h made lignin colloids more stable. The thermal treatment slightly disrupted the structure of colloids and caused aggregation of a few colloidal particles, resulting in the multimodal distribution in ATSL medium. While mixing for 30 min had not achieved a stable state for lignin colloids, TSL medium showed lower resistance to the thermal sterilization. As a result, most of the colloidal lignin particles aggregated in TSL medium, leading to a relatively larger and uniform lignin particle size. Therefore, DLS and precipitation results were consistent with the analysis based on pH changes and light transmittance of different mediums. Hence, thermal sterilization caused the aggregation of colloidal lignin particles, which increased the lignin particles size and even led to precipitation. Besides, prolonging the mixing period at alkaline conditions helped make the lignin colloid structure more stable and more resistant to thermal treatment. Overall, DLS results revealed that colloidal lignin particle size in ASL medium showed a narrow distribution, of which

the hydrodynamic radius at the peak was 15 nm while the size of most bacteria was 200-1000 nm in radius and 500-5000 nm in length.[67] Moreover, there was no precipitate generation during the alkali sterilization process compared with the conventional thermal treatment. These results suggest that lignin dispersion in ASL medium might no longer be the limiting factor for microbial lignin conversion. Alkali sterilization for 24 h in ASL medium achieved complete sterilization, reduced colloidal lignin particle size, and avoided precipitation, which should facilitate microbial lignin conversion.

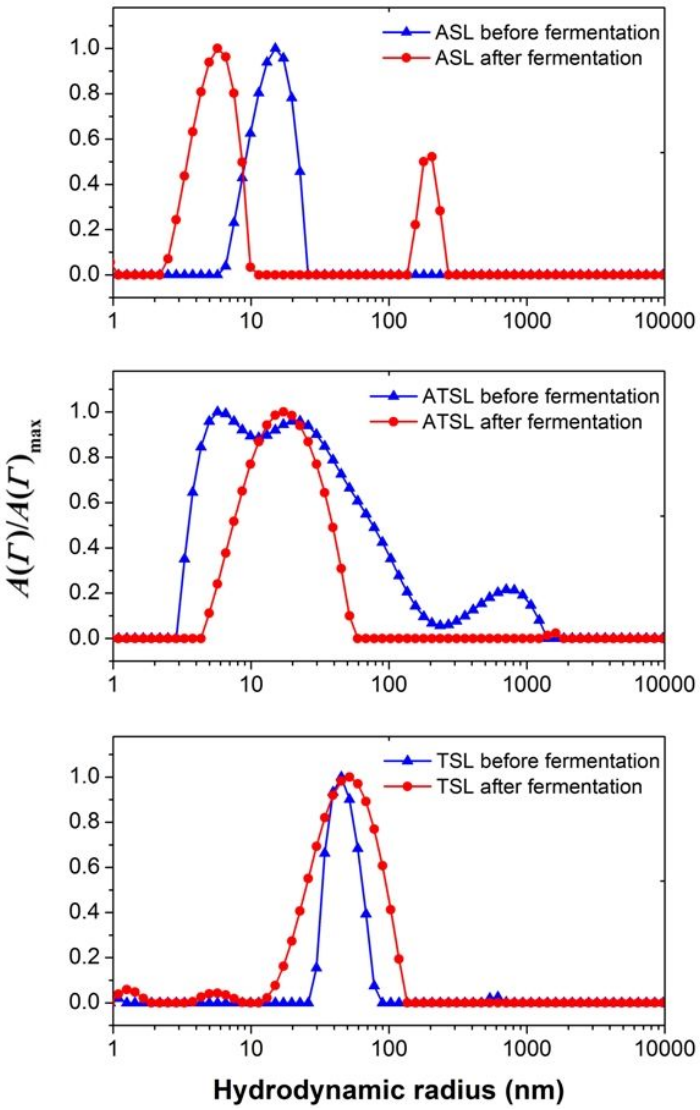

Fig. 3 Comparison of colloidal lignin hydrodynamic size distributions in different mediums before and after fermentation.

3.3 Lignin molecular weight and structure alterations during sterilization

treatment

Along with colloidal lignin particle size analysis, the effects of different sterilization strategies on lignin molecular weight were also investigated. As shown in Fig. 4, both weight-average molecular weight (M_w) and molar-mass dispersity ($Đ_M$) decreased following the order of RKL (raw Kraft lignin) > NSL > ASL. In particular, M_w of RKL decreased from 2221 g/mol to 929 g/mol in ASL. These phenomena implied that alkaline sterilization treatment reduced lignin molecular weight while improving its homogeneity. Qian et al.[63] investigated the influence of pH on lignin (i.e., sodium lignosulfonate) molecular weight systematically. It was reported that M_w of lignin decreased with increasing solution pH due to the higher ionization degree of carboxylic acid and phenolic hydroxyl groups, which was consistent with the results in the present study.[63] As for thermal sterilization treatment, it demonstrated a relatively complex effect on lignin molecular structure depending on the lignin substrates. For low M_w lignin such as ASL, thermal sterilization caused a slight increase of M_w from 929 to 986 g/mol in the ATSL medium. While for lignin with higher M_w (NSL), the thermal sterilization decreased lignin M_w from 1432 to 1207 g/mol in TSL. These results suggest that depolymerization and repolymerization reactions might occur simultaneously during the thermal sterilization process.[47-49] For ATSL, due to the initial lower M_w and smaller lignin fragments, repolymerization reactions might be stronger than the depolymerization, resulting in a slight increase M_w by 6.1% and a $Đ_M$ increase by 15.6% during the thermal sterilization. While for TSL, depolymerization reactions were stronger than repolymerization due to the higher molecular weight of lignin substrates, leading to that M_w and $Đ_M$ decreased by 15.7% and 5.5%, respectively. Brosse et al.[48] reported that M_w of milled wood lignin decreased from 5510 to 4020 g/mol, and $Đ_M$ decreased from 1.49 to 1.44 during a thermal treatment at 230 °C for 7 h, presenting a decrease by 27.0% for M_w and a 3.4% decrease for $Đ_M$, respectively. Kacik et al.[47] further investigated pinewood lignin structure alterations during the heat sterilization at 120 °C for 10 h. Results suggested that the cleavage of alkyl-aryl ether bonds and demethoxylation might occur during the thermal treatment process.[47,48] Since lignin

precipitates accounted for 20.5% weight (Table 1) in TSL medium, lignin molecular weights in both supernatant (TSL-S) and precipitates (TSL-P) were further compared. Fig. 4 shows that M_w of TSL-S and TSL-P were 1161 and 3724 g/mol, respectively. $Đ_M$ value of TSL-S and TSL-P were 5.38 and 3.99, respectively. These results indicated a significant variation of lignin molecular structure caused by the thermal sterilization treatment. It is interesting to note that although M_w of TSL was lower than that of NSL, a notable amount of lignin was precipitated in TSL medium while none was detected in NSL. This phenomenon reveals that thermal sterilization caused particle aggregation, especially for TSL medium with a short alkaline treatment. Therefore, thermal sterilization presented multiple effects on the lignin-containing medium: altering lignin chemical structure and facilitating aggregation of colloidal lignin particles. These various physical and chemical properties of lignin mediums after different sterilization treatments could further influence the biological lignin valorization efficiency.

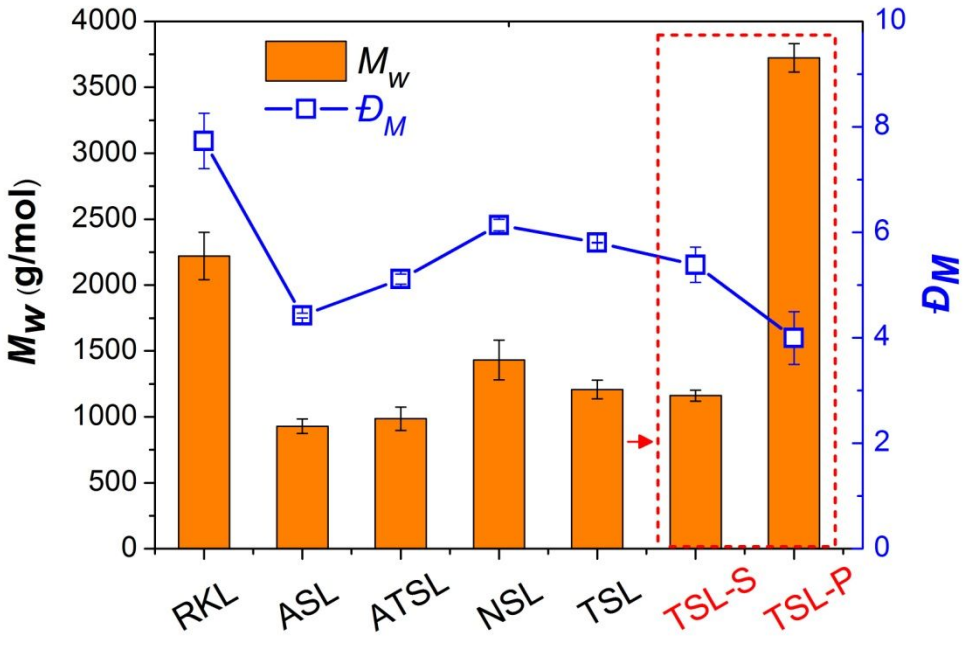

Fig. 4 Comparison of weight-average molecular weight (M_w) and molar-mass dispersity ($Đ_M$) of lignin from different sterilization treatments. RKL: raw Kraft lignin, ASL: alkaline sterilized lignin, ATSL: alkaline and thermally sterilized lignin, NSL: non-sterilized lignin, TSL: thermally sterilized lignin. TSL-S and TSL-P represent lignin

from supernatant and precipitates of TSL medium, respectively. The data represent the average of two replicates. Error bars represent standard deviations.

HSQC NMR was applied to investigate the lignin interunit linkage changes during those sterilization treatments. As shown in Fig. 5, *β*-O-4, *β*-*β*, *β*-5 interunit linkages were observed in all samples after different sterilization treatments. Since the low molecular weight of RKL substrates (2221 g/mol) were applied in the present study, most of the interunit linkages had already been cleaved during the Kraft pulping process, leaving relatively low contents of *β*-O-4, *β*-*β*, *β*-5 linkages.[68] It is noted that the relative content of *β*-O-4 linkage in TSL decreased by 4.05% than that in NSL while the relative content of *β*-O-4 linkage in ATSL was 3.55% higher than that in ASL (Fig. 5c). These results showed similar changing trends with lignin M_w during the thermal sterilization processes. The ^{31}P NMR data summarized in Fig. 5d indicated that the carboxylic acid contents in ASL and ATSL reached 0.60 mmol/g lignin, which was 50% higher than those of NSL and TSL. These results were in agreement with the pH changing trend as well as the colloidal lignin particle size distribution. During the alkaline sterilization process, more carboxylic acid groups were reacted with OH^- as shown in equation (3), leading to the pH decrease and more negatively charged lignin colloid structure. These results further prevented lignin particle aggregation and resulted in a smaller particle size. Overall, ASL presented the lowest lignin M_w of 929 g/mol and most uniform lignin distribution among these fermentation mediums, which should benefit microbial utilization.[10,35]

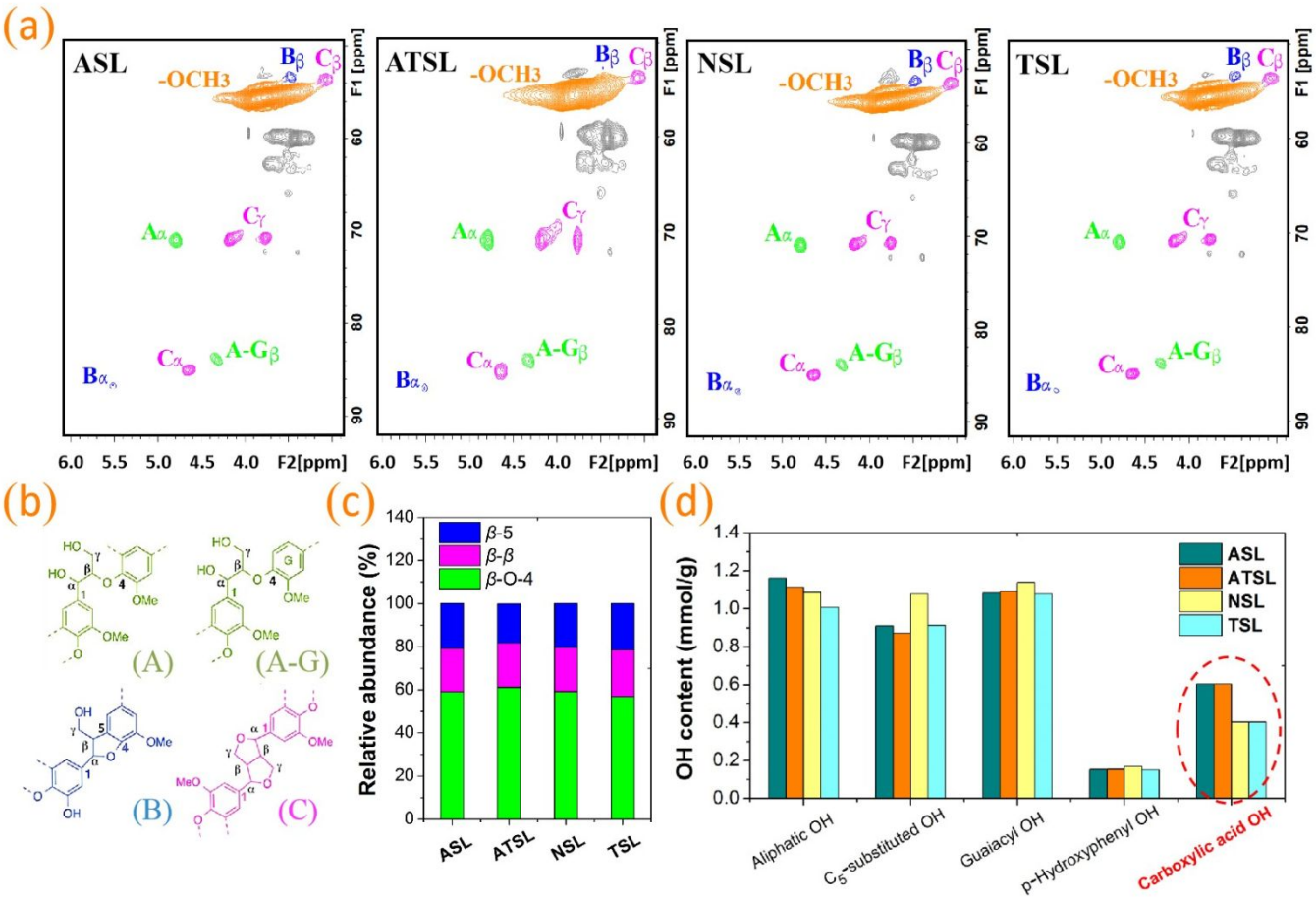

Fig. 5 NMR characterization of lignin with different sterilization treatments. (a) Aliphatic region of HSQC NMR spectra. (b) Main substructures identified: (A) *β*-O-4-aryl ether, (A-G) *β*-O-4-guaiacyl unit, (B) *β*-5-phenylcoumaran, (C) *β*-*β*-resinol linkages. (c) Relative abundance of lignin interunit linkages. (d) Quantification of different hydroxyl group contents determined by ^{31}P NMR spectra.

3.4 *R. opacus* PD630 cell growth and lipids production

In order to examine the effects of different sterilization methods on fermentation performance, PD630 cell growth, lipids production, and lignin degradation were systematically compared. It was found that microbes showed various growth and metabolism behaviors on different sterilized mediums (Fig. 6a). These results suggested that the medium property alterations by different sterilization treatments influenced the lignin fermentation performance significantly. Microbes grew slowly in the early fermentation stage (1-3 d), which should be attributed to microbial cells' adaption process to the culturing environment during this lag phase. Nevertheless, the cell

amount in ASL medium was the highest during this stage. The smaller particles and lower lignin molecular weight of ASL could be easily accessed by microbial cells and thus shorten the microbial adaption period. PD630 cells presented a faster growth as fermentation continued in all samples. After fermentation for 7 d, cell amounts in ASL, ATSL, and TSL mediums reached 9.0×10^6, 7.2×10^6, and 2.2×10^6 CFU/mL, respectively. It is worth noting that cell amounts in ASL and ATSL mediums were always higher than that in TSL medium during the whole fermentation period. Accordingly, cell amounts in ASL and ATSL mediums after fermentation were 4.1 and 3.3 times that in TSL medium, respectively. The results could be due to that prolonging mixing time under alkaline environment during the sterilization stage improved lignin medium properties and thus benefited microbial growth.

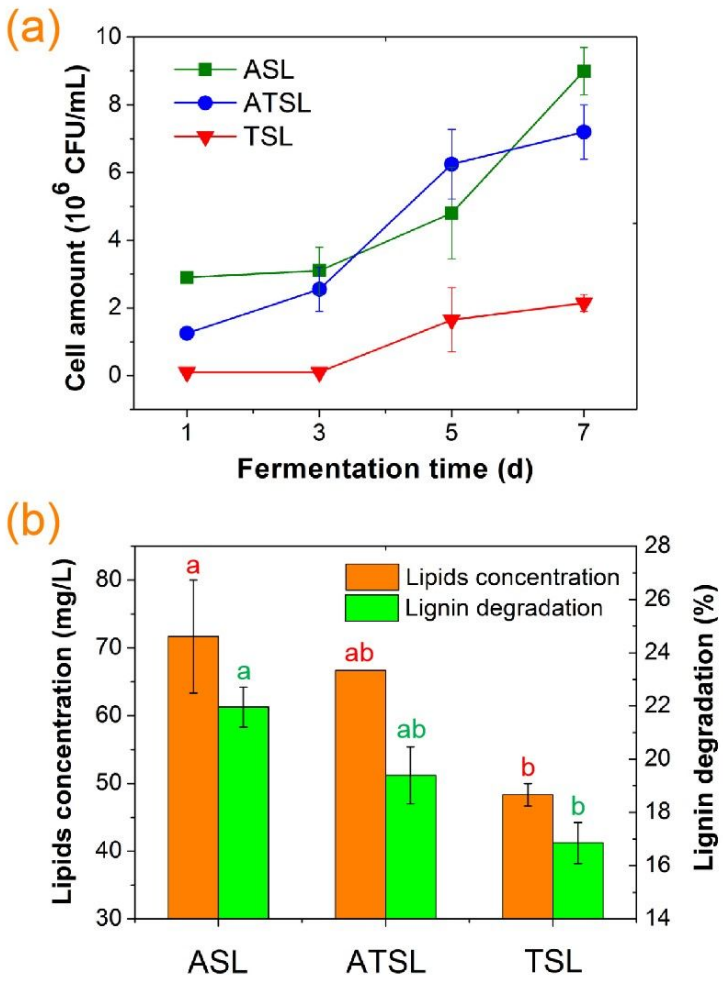

Fig. 6 Comparison of microbial growth curves of *R. opacus* PD630 (a), lipids

production, and lignin degradation (b) during fermentation on different mediums. The data represent the average of two replicates. Error bars represent standard deviations. Bars followed by different letters show significant difference (P<0.05) according to the Duncan's multiple range test.

Lignin degradation and lipids production during fermentation on different mediums were also compared to investigate lignin properties' influence on microbial metabolism. Fig. 6b shows that lignin degradation and lipids production increased in the order of TSL < ATSL < ASL, which presented a similar trend as microbial cell growth. In detail, lignin degradation percents were 22.0%, 19.4%, and 16.9% during fermentation on ASL, ATSL, and TSL mediums, respectively. Yang et al.[16,54] reported that the insufficient extracellular lignin depolymerization activity to produce reactive lignin intermediates was one of the main factors limiting lignin utilization by PD630. The smaller particles and lower lignin molecular weight of ASL should make the depolymerization process relatively easier and promote microbial utilization. As a result, lipids concentration in ASL medium reached 71.7 mg/L, which was 48.3% and 7.5% higher than those in TSL and ATSL mediums, respectively. These results confirmed that the improved lignin properties of ASL facilitated microbial growth and metabolism. It was noted that the cells growth increase presented a higher fold as compared to the lipids yield, which was also observed in a previous study by Xie et al.[69] This phenomenon could be due to the larger variation in measuring lipids yield using weight-based methods at the low lipid titer on unimproved lignin medium.[69] Nevertheless, PD630 cell amount, lipids production, and lignin degradation all increased following the order of TSL < ATSL < ASL, confirming that alkaline treatment improved lignin fermentation performance. It could be concluded that ASL without thermal treatment achieved complete sterilization, modified lignin properties, and enhanced fermentation performance significantly, proving that alkali sterilization is an effective strategy to facilitate biological lignin valorization.

3.5 Lignin properties changes during fermentation process

3.5.1 Variations of colloidal lignin particle size distribution

In order to gain a more comprehensive understanding of the lignin utilization process by PD630 with different sterilization treatments, lignin property variations during fermentation were investigated systematically on different mediums. As shown in Fig. 3, different mediums presented various changing behaviors of colloidal lignin particle size during fermentation, suggesting various microbial activities within these mediums. The peak of ASL medium was split during the fermentation process. The main peak shifted left while the other one appeared on the right compared with the original peak. The primary peak shifted to left, indicating that most of the lignin particles were disrupted by the microbial metabolism, resulting in a decreased particle size. While the other relatively low peak appeared on the right, demonstrating that a small part of lignin particles aggregated due to the altered lignin structure during the fermentation process. As for ATSL medium, the colloidal lignin particle size presented a wide distribution before fermentation. Since the small particles were easier to be utilized by microbes, the left peak disappeared after fermentation. While the right low peak also disappeared, indicating that the microbial metabolism also caused larger particles damage during the fermentation. Comparing with ASL and ATSL, colloidal lignin particle size distribution in TSL changed slightly during the fermentation process, which may be due to the relatively weak microbial activities within this medium. Nevertheless, the peak of TSL medium showed a broadening trend during the fermentation. On one hand, the particles were destroyed by microbial cells, resulting in that some particles became smaller and even hydrodynamic radius less than 10 nm. On the other hand, some particles aggregated during the fermentation process, leading to the appearance of larger lignin particles. These behaviors were similar to ASL. However, since the volume of lignin particles in TSL medium before fermentation was 27-fold larger than that in ASL, microbial activities in TSL were much weaker, presenting a relatively slighter change in lignin particle size distribution. Therefore, these results suggest that the colloidal lignin particle size presented a significant influence on fermentation. Alkaline sterilization strategy can produce much smaller lignin particles and thus benefit microbial utilization.

3.5.2 Variations of lignin M_w and major aromatics metabolites

Besides lignin particles size, variations of lignin molecular structure and the content of primary metabolites during fermentation were investigated to evaluate the microbial metabolism within different mediums. Fig. 7 shows that M_w of lignin increased rapidly while $Đ_M$ decreased fast during the first day of fermentation. This result can be interpreted as that lignin with lower molecular weight was utilized preferentially by microbes, leaving the high molecular weight fraction in the medium during this initial stage.[70] After that, M_w began to decrease while $Đ_M$ increased during 1-3 d, implying the degradation of high molecular weight lignin through microbial metabolism to produce fragments. It has been reported that PD630 could secrete lignin degradation-related enzyme (e.g., catalase-peroxidase), by which lignin can be degraded into monomers and oligomers.[16] These lignin derivatives can be further converted to smaller aromatics (e.g., vanillin) for further catabolism via various metabolic routes such as β-ketoadipate (β-KAP), phenylacetic acid (PAA), and homogentisate pathways.[10,16,70] During fermentation period of 3-7 d, M_w and $Đ_M$ presented relatively stable trends, indicating that lignin degradation, as well as the generated fragments consumption by microbes, reached nearly equilibrium state. Overall, M_w and $Đ_M$ of ASL were lower than those of ATSL and TSL during the fermentation process, representing a relatively uniform lower molecular weight lignin in ASL, which facilitated the microbial growth and metabolism.

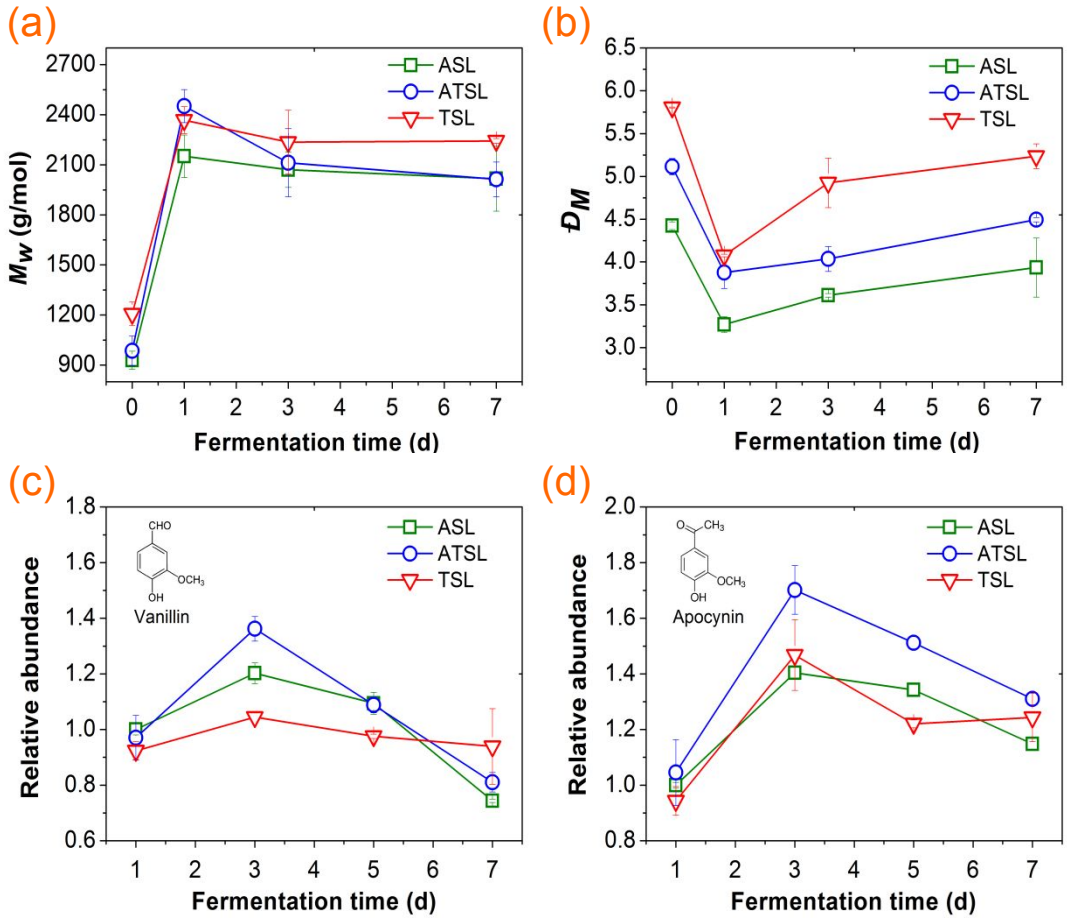

Fig. 7 Lignin molecular weight (a), molar-mass dispersity (b), and significant aromatic monomer metabolites contents (c and d) variations during fermentation in different mediums. The data represent the average of two replicates. Error bars represent standard deviations.

Vanillin and apocynin were detected in mediums during fermentation, while vanillin showed a much higher peak than apocynin in GC-MS determination, suggesting that vanillin was a significant metabolite in Kraft lignin derivation process by PD630. Fig. 7c shows that vanillin abundance increased during 1-3 d of fermentation, indicating that lignin degradation became the major activity within this stage. The result was consistent with the analysis of M_w changing behaviors. Reactive aromatics were generated and accumulated during the fermentation for 1-3 d and then were consumed rapidly as the fermentation continued. By comparing vanillin abundance changes with PD630 growth curves after fermentation for 3 d, it was interesting to note that the changing trends of these two items were closely relevant. For example, during the

fermentation period of 3-5 d, vanillin content in ATSL medium presented the largest decline while the decreasing degree in ASL and TSL mediums were almost the same. Accordingly, it was noted that PD630 cell growth in ATSL medium presented the fastest increase compared with those in ASL and TSL mediums during fermentation of 3-5 d (Fig. 6a). Besides, the microbial growth in ASL and TSL mediums showed a similar increasing speed within this stage. As fermentation continued from 5 to 7 d, vanillin content decreasing extent followed the order of ASL > ATSL > TSL, which showed a similar trend of the cell amount increasing speed. The close relationship between vanillin content and microbial cell amount confirmed that vanillin was a key metabolite during Kraft lignin fermentation by PD630. Meanwhile, apocynin abundance (Fig. 7d) presented a similar changing behavior as vanillin during the fermentation process. These results suggest that the medium's reactive aromatics contents played a significant role in determining lignin fermentation efficiency. Expanding reactive aromatics capacity either by tailoring lignin chemistry or upgrading microbial strains, represent promising ways to improve biological lignin valorization in the future study.[18]

3.6 Proposed mechanisms of enhancing lignin bioconversion by alkali sterilization

The mechanisms of enhanced biological lignin valorization by alkali sterilization were proposed in the present study based on aforementioned the characterization of lignin and the fermentation performance using PD630. As shown in Fig. 8, different sterilization treatments presented significant influences on lignin properties and further influenced fermentation performance. On the one hand, TSL caused 20.5% (weight percent) lignin precipitates while the other parts of lignin aggregated as large colloidal particles. As opposed to the thermal treatment, alkali sterilization did not cause lignin precipitation. Moreover, the volume of colloidal lignin particles in ASL medium reduced by around 96.3% compared with those in TSL due to the enhanced ionization of acidic groups (i.e., carboxylic acid groups). These results demonstrated that alkali sterilization improved lignin distribution in the medium, providing more uniform accessible substrates for microbial cells. On the other hand, from the viewpoints of

lignin molecular structure, M_w and $Đ_M$ of ASL decreased by 23.0% and 23.8%, respectively, compared to those in TSL. The uniform lower molecular weight lignin of ASL was easier to be degraded and converted to reactive aromatics (e.g., vanillin), making it easier for microbial utilization. As a result, PD630 cell amount was promoted, lignin degradation was enhanced, and lipids production was improved using ASL as a carbon source, which increased by 309%, 30.3%, and 48.3%, respectively, as compared with those in TSL medium. Therefore, alkali sterilization reduced lignin molecular and colloidal particle size, and thus provided more accessible and readily degraded lignin substrates for microbes, which promoted PD630 cell growth and lipids production effectively. Furthermore, alkali sterilization strategy integrates alkaline solubilization and sterilization as a unit operation, by which thermal sterilization is canceled. Not only steam is saved but also fermentors no longer need to withstand high temperature and pressure, which simplify operation and show great potentials in large scale lignin fermentation.

Fig. 8 Proposed model for elucidating the mechanisms of enhanced lignin bioconversion by alkali sterilization. Sample information was presented in Fig. 1.

4. Conclusions

In summary, we have presented a novel alkali sterilization strategy for lignin

medium to replace thermal treatment, which facilitated lignin dispersion and promoted fermentation performance significantly. Alkali sterilization enhanced the ionization process of acidic groups in lignin colloids, reducing volume of colloidal lignin particles by 96.3% compared with the conventional thermal sterilization. Besides, there was no precipitate generation during alkali sterilization process. Moreover, alkali sterilization reduced lignin molecular weight and molar-mass dispersity by 23.0% and 23.8%, respectively. Through providing more uniformly distributed and readily degraded lignin substrates, alkali sterilization strategy facilitated both *R. opacus* PD630 growth and lipids production efficiently. This work presents a facile and effective strategy to overcome inhomogeneous lignin distribution in aqueous mediums, showing great potentials as a platform sterilization technique to promote biological lignin valorization.

Conflicts of interest

There are no conflicts to declare.

Acknowledgments

The authors thank the National Natural Science Foundation of China (21706136), the Natural Science Foundation of Inner Mongolia (2019MS02026), and the China Scholarship Council for support. In addition, this manuscript has been authored (AJR, YP) in part, by UT-Battelle, LLC under Contract No. DE-AC05-00OR22725 with the U.S. Department of Energy. The United States Government retains and the publisher, by accepting the article for publication, acknowledges that the United States Government retains a non-exclusive, paid-up, irrevocable, world-wide license to publish or reproduce the published form of this manuscript, or allow others to do so, for United States Government purposes. The Department of Energy will provide public access to these results of federally sponsored research in accordance with the DOE Public Access Plan (http://energy.gov/downloads/doe-public-access-plan). The views and opinions of the authors expressed herein do not necessarily state or reflect those of

the United States Government or any agency thereof. Neither the United States Government nor any agency thereof, nor any of their employees, makes any warranty, expressed or implied, or assumes any legal liability or responsibility for the accuracy, completeness, or usefulness of any information, apparatus, product, or process disclosed, or represents that its use would not infringe privately owned rights.

References

1 A. J. Ragauskas, G. T. Beckham, M. J. Biddy, R. Chandra, F. Chen, M. F. Davis, B. H. Davison, R. A. Dixon, P. Gilna, M. Keller, P. Langan, A. K. Naskar, J. N. Saddler, T. J. Tschaplinski, G. A. Tuskan and C. E. Wyman, *Science*, 2014, **344**, 1246843.

2 M. Kumar, S. You, J. Beiyuan, G. Luo, J. Gupta, S. Kumar, L. Singh, S. Zhang and D. C. W. Tsang, *Bioresour. Technol.*, 2020, **320**, 124412.

3 C. Li, X. Zhao, A. Wang, G. W. Huber and T. Zhang, *Chem. Rev.*, 2015, **115**, 11559-11624.

4 G. Wang, T. Pang, S. Chen, W. Sui, C. Si and Y. Ni, *Green Chem.*, 2020, **22**, 8594-8603.

5 M. Garedew, F. Lin, B. Song, T. M. DeWinter, J. E. Jackson, C. M. Saffron, C. H. Lam and P. T. Anastas, *ChemSusChem*, 2020, **13**, 4214-4237.

6 S. Hong, X. J. Shen, Z. Xue, Z. Sun and T. Q. Yuan, *Green Chem.*, 2020, **22**, 7219-7232.

7 R. E. Davis, N. J. Grundl, L. Tao, M. J. Biddy, E. C. Tan, G. T. Beckham, D. Humbird, D. N. Thompson and M. S. Roni, *Process Design and economics for the conversion of lignocellulosic biomass to hydrocarbon fuels and coproducts: 2018 biochemical design case update; biochemical deconstruction and conversion of biomass to fuels and products via integrated biorefinery pathways*, National Renewable Energy Lab. (NREL), Golden, CO (United States), 2018.

8 R. Shen, L. Tao and B. Yang, *Biofuels Bioprod. Biorefin.*, 2019, **13**, 486-501.

9 M. M. Abu-Omar, K. Barta, G. T. Beckham, J. S. Luterbacher, J. Ralph, R. Rinaldi, Y. Román-Leshkov, J. S. Samec, B. F. Sels and F. Wang, *Energy Environ. Sci.*, 2021, **14**, 262-292.

10 Z. M. Zhao, Z. H. Liu, Y. Pu, X. Meng, J. Xu, J. S. Yuan and A. J. Ragauskas, *ChemSusChem*, 2020, **13**, 5423-5432.

11 J. Ralph, C. Lapierre and W. Boerjan, *Curr. Opin. Biotechnol.*, 2019, **56**, 240-249.

12 Z. H. Liu, R. K. Le, M. Kosa, B. Yang, J. Yuan and A. J. Ragauskas, *Renew. Sustainable Energ. Rev*, 2019, **105**, 349-362.

13 X. Wu, X. Fan, S. Xie, J. Lin, J. Cheng, Q. Zhang, L. Chen and Y. Wang, *Nat. Catal.*, 2018, **1**, 772-780.

14 D. Salvachúa, A. Z. Werner, I. Pardo, M. Michalska, B. A. Black, B. S. Donohoe, S. J. Haugen, R. Katahira, S. Notonier, K. J. Ramirez, A. Amore, S. O. Purvine, E. M. Zink, P. E. Abraham,

R. J. Giannone, S. Poudel, P. D. Laible, R. L. Hettich and G. T. Beckham, *Proc. Natl. Acad. Sci. U. S. A.*, 2020, **117**, 9302-9310.

15 C. Zhao, S. Xie, Y. Pu, R. Zhang, F. Huang, A. J. Ragauskas and J. S. Yuan, *Green Chem.*, 2016, **18**, 1306-1312.

16 X. Li, Y. He, L. Zhang, Z. Xu, H. Ben, M. J. Gaffrey, Y. Yang, S. Yang, J. S. Yuan, W. J. Qian and B. Yang, *Biotechnol. Biofuels*, 2019, **12**, 60.

17 Z. Wang, N. Li and X. Pan, *Fuel*, 2019, **240**, 119-125.

18 S. Xie, S. Sun, F. Lin, M. Li, Y. Pu, Y. Cheng, B. Xu, Z. Liu, L. da Costa Sousa, B. E. Dale, A. J. Ragauskas, S. Y. Dai and J. S. Yuan, *Adv. Sci.*, 2019, **6**, 1801980.

19 R. K. Le, T. Wells Jr, P. Das, X. Meng, R. J. Stoklosa, A. Bhalla, D. B. Hodge, J. S. Yuan and A. J. Ragauskas, *RSC Adv.*, 2017, **7**, 4108-4115.

20 D. Salvachúa, T. Rydzak, R. Auwae, A. De Capite, B. A. Black, J. T. Bouvier, N. S. Cleveland, J. R. Elmore, A. Furches, J. D. Huenemann, R. Katahira, W. E. Michener, D. J. Peterson, H. Rohrer, D. R. Vardon, G. T. Beckham and A. M. Guss, *Microb. Biotechnol.*, 2020, **13**, 290-298.

21 Z. Xu, M. Xu, C. Cai, S. Chen and M. Jin, *Bioresour. Technol.*, 2021, **319**, 124210.

22 R. Morya, A. Sharma, M. Kumar, B. Tyagi, S. S. Singh and I. S. Thakur, *Bioresour. Technol.*, 2020, **320**, 124439.

23 Z. H. Liu, S. Shinde, S. Xie, N. Hao, F. Lin, M. Li, C. G. Yoo, A. J. Ragauskas and J. S. Yuan, *Sustain. Energ. Fuels*, 2019, **3**, 2024-2037.

24 T. Sonoki, K. Takahashi, H. Sugita, M. Hatamura, Y. Azuma, T. Sato, S. Suzuki, N. Kamimura and E. Masai, *ACS Sustainable Chem. Eng.*, 2018, **6**, 1256-1264.

25 C. Cai, Z. Xu, M. Xu, M. Cai and M. Jin, *ACS Sustainable Chem. Eng.*, 2020, **8**, 2016-2031.

26 D. Salvachúa, C. W. Johnson, C. A. Singer, H. Rohrer, D. J. Peterson, B. A. Black, A. Knapp and G. T. Beckham, *Green Chem.*, 2018, **20**, 5007-5019.

27 A. Chatterjee, D. M. DeLorenzo, R. Carr and T. S. Moon, *Curr. Opin. Biotechnol.*, 2020, **64**, 10-16.

28 X. Li and Y. Zheng, *Biotechnol. Prog.*, 2020, **36**, e2922.

29 S. Xie, A. J. Ragauskas and J. S. Yuan, *Ind. Biotechnol.*, 2016, **12**, 161-167.

30 L. Xu, S. J. Zhang, C. Zhong, B. Z. Li and Y. J. Yuan, *Ind. Eng. Chem. Res.*, 2020, **59**, 16923-16938.

31 E. Mahdinia, D. Cekmecelioglu and A. Demirci, in *Essentials in Fermentation Technology*, Springer, 2019, pp. 213-236.

32 Z. M. Zhao, L. Wang and H. Z. Chen, *Bioresour. Technol.*, 2016, **203**, 204-210.

33 B. Li, S. You, W. Qi, Y. Wang, R. Su and Z. He, *Eur. Polym. J.*, 2020, **126**, 109539.

34 S. Maitz, W. Schlemmer, M. A. Hobisch, J. Hobisch and M. Kienberger, *Adv. Sustain. Syst.*, 2020, 2000052.

35 G. T. Beckham, C. W. Johnson, E. M. Karp, D. Salvachúa and D. R. Vardon, *Curr. Opin. Biotechnol.*, 2016, **42**, 40-53.

36 T. Y. Nguyen, C. M. Cai, R. Kumar and C. E. Wyman, *Proc. Natl. Acad. Sci. U. S. A.*, 2017, **114**, 11673-11678.

37 T. Y. Nguyen, C. M. Cai, O. Osman, R. Kumar and C. E. Wyman, *Green Chem.*, 2016, **18**, 1581-1589.

38 X. Meng, A. Parikh, B. Seemala, R. Kumar, Y. Pu, P. Christopher, C. E. Wyman, C. M. Cai and A. J. Ragauskas, *ACS Sustainable Chem. Eng.*, 2018, **6**, 8711-8718.

39 Z. H. Liu, S. Xie, F. Lin, M. Jin and J. S. Yuan, *Biotechnol. Biofuels*, 2018, **11**, 21.

40 Z. H. Liu, M. L. Olson, S. Shinde, X. Wang, N. Hao, C. G. Yoo, S. Bhagia, J. R. Dunlap, Y. Pu, K. C. Kao, A. J. Ragauskas, M. Jin and J. S. Yuan, *Green Chem.*, 2017, **19**, 4939-4955.

41 S. Sun, F. Liu, L. Zhang and X. Fan, *Ind. Crop Prod.*, 2018, **119**, 260-266.

42 S. Sun, L. Zhang, F. Liu, X. Fan and R. C. Sun, *Biotechnol. Biofuels*, 2018, **11**, 137.

43 G. Wang and H. Chen, *Sep. Purif. Technol.*, 2013, **105**, 98-105.

44 L. Lin, Y. Cheng, Y. Pu, S. Sun, X. Li, M. Jin, E. A. Pierson, D. C. Gross, B. E. Dale, S. Y. Dai, A. J. Ragauskas and J. S. Yuan, *Green Chem.*, 2016, **18**, 5536-5547.

45 A. Rodriguez, D. Salvachúa, R. Katahira, B. A. Black, N. S. Cleveland, M. Reed, H. Smith, E. E. Baidoo, J. D. Keasling, B. A. Simmons, G. T. Beckham and J. M. Gladden, *ACS Sustainable Chem. Eng.*, 2017, **5**, 8171-8180.

46 Z. M. Zhao, L. Wang and H. Z. Chen, *Bioresour. Technol.*, 2015, **192**, 547-555.

47 F. Kacik, J. Luptáková, P. Šmíra, A. Nasswettrová, D. Kačíková and V. Vacek, *BioRes.*, 2016, **11**, 3442-3452.

48 N. Brosse, R. El Hage, M. Chaouch, M. Pétrissans, S. Dumarçay and P. Gérardin, *Polym. Degrad. Stab.*, 2010, **95**, 1721-1726.

49 J. Y. Kim, H. Hwang, S. Oh, Y. S. Kim, U. J. Kim and J. W. Choi, *Int. J. Biol. Macromol.*, 2014, **66**, 57-65.

50 B. Setlow, C. Loshon, P. Genest, A. Cowan, C. Setlow and P. Setlow, *J. Appl. Microbiol.*, 2002, **92**, 362-375.

51 D. Valverde García, É. Pérez Esteve and J. M. Barat Baviera, *Compr. Rev. Food Sci. Food Saf.*, 2020, **19**, 2200-2221.

52 A. P. M. Pereira, H. A. Stelari, F. Carlin and A. S. Sant'Ana, *LWT*, 2019, **111**, 394-400.

53 Y. Y. Wang, M. Li, C. E. Wyman, C. M. Cai and A. J. Ragauskas, *ACS Sustainable Chem. Eng.*, 2018, **6**, 6064-6072.

54 Y. He, X. Li, H. Ben, X. Xue and B. Yang, *ACS Sustainable Chem. Eng.*, 2017, **5**, 2302-2311.

55 J. L. Davis, X. Wang, K. Bornani, J. P. Hinestrosa, J. W. Mays and S. M. Kilbey, *Macromolecules*, 2016, **49**, 2288-2297.

56 J. P. Hinestrosa, J. Alonzo, M. Osa and S. M. Kilbey, *Macromolecules*, 2010, **43**, 7294-7304.

57 X. Wang, J. L. Davis, J. P. Hinestrosa, J. W. Mays and S. M. Kilbey, *Macromolecules*, 2014, **47**, 7138-7150.

58 A. Sluiter, B. Hames, R. Ruiz, C. Scarlata, J. Sluiter, D. Templeton and D. Crocker, *Determination of structural carbohydrates and lignin in biomass*, National Renewable Energy

Lab. (NREL), Golden, CO (United States), 2008.

59 S. Zhang, M. Li, N. Hao and A. J. Ragauskas, *ACS Omega*, 2019, **4**, 20197-20204.

60 X. Meng, C. Crestini, H. Ben, N. Hao, Y. Pu, A. J. Ragauskas and D. S. Argyropoulos, *Nat. Protoc.*, 2019, **14**, 2627-2647.

61 X. Meng, A. Parikh, B. Seemala, R. Kumar, Y. Pu, C. E. Wyman, C. M. Cai and A. J. Ragauskas, *Bioresour. Technol.*, 2019, **272**, 202-208.

62 J. M. Halpern, C. A. Gormley, M. A. Keech and H. A. Von Recum, *J. Mater. Chem. B*, 2014, **2**, 2764-2772.

63 Y. Qian, Y. Deng, C. Yi, H. Yu and X. Qiu, *BioRes.*, 2011, **6**, 4686-4695.

64 W. Zhao, B. Simmons, S. Singh, A. J. Ragauskas and G. Cheng, *Green Chem.*, 2016, **18**, 5693-5700.

65 M. Zawadzki, T. Runge and A. J. Ragauskas, *J. Pulp Pap. Sci.*, 2000, **26**, 102-106.

66 H. Zhang, Y. Bai, B. Yu, X. Liu and F. Chen, *Green Chem.*, 2017, **19**, 5152-5162.

67 H. Zheng, Y. Bai, M. Jiang, T. A. Tokuyasu, X. Huang, F. Zhong, Y. Wu, X. Fu, N. Kleckner, T. Hwa and C. Liu, *Nat. Microbiol.*, 2020, **5**, 995-1001.

68 C. Fernández-Costas, S. Gouveia, M. Sanromán and D. Moldes, *Biomass Bioenergy*, 2014, **63**, 156-166.

69 S. Xie, Q. Sun, Y. Pu, F. Lin, S. Sun, X. Wang, A. J. Ragauskas and J. S. Yuan, *ACS Sustainable Chem. Eng.*, 2017, **5**, 2215-2223.

70 Z. Wei, G. Zeng, F. Huang, M. Kosa, D. Huang and A. J. Ragauskas, *Green Chem.*, 2015, **17**, 2784-2789.